

AD-A103 903 NATIONAL AERONAUTICS AND SPACE ADMINISTRATION MOFFET--ETC FG 20/4
DYNAMIC BEHAVIOR OF AN UNSTEADY TURBULENT BOUNDARY LAYER.(U)
JUL 81 P G PARikh, W C REYNOLDS, R JAYARAMAN

UNCLASSIFIED NASA-A-6640

NASA-TM-81304

NL



ADA103903

LEVEL ✓

C

S

Jan 14, 1982

100-1000

Dynamic Behavior of an Unsteady Turbulent Boundary Layer

P. G. Parikh, W. C. Reynolds,
R. Jayaraman and L. W. Carr

DTIC
ELECTE
SEP 8 1981
S D
H

July 1981

FILE COPY



National Aeronautics and
Space Administration

Ames Research Center
Moffett Field, California 94035

SD



United States Army
Aviation Research
and Development
Command



81 9 08 69

Dynamic Behavior of an Unsteady Turbulent Boundary Layer

P. G. Parikh,

W. C. Reynolds,

R. Jayaraman, Department of Mechanical Engineering
Stanford University, Stanford, California

L. W. Carr, Aeromechanics Laboratory

AVRADCOM Research and Technology Laboratories
Ames Research Center, Moffett Field, California

DTIC
SELECTED
SEP 8 1981
S D H

DISTRIBUTION STATEMENT A
Approved for public release:
Distribution Unlimited

NASA
National Aeronautics and
Space Administration

United States Army
Aviation Research
and Development
Command



DYNAMIC BEHAVIOR OF AN UNSTEADY TURBULENT BOUNDARY LAYER

BY

P.G. PARIKH, W.C. REYNOLDS, R. JAYARAMAN,
Department of Mechanical Engineering
Stanford University

AND

L. W. CARR
U.S. Army Aeromechanics Laboratory
Moffett Field, Ca

Presented at the IUTAM Symposium on
UNSTEADY TURBULENT SHEAR FLOWS
5-8 May, 1981
TOULOUSE, FRANCE

-iii-

Accesnion for	DTIS	CRAB	<input type="checkbox"/>
DTIC	TEB	Unannounced	<input type="checkbox"/>
Justification			
By	Distribution		
Availability Code			
All and as			
Dist	Special		

DYNAMIC BEHAVIOR OF AN UNSTEADY TURBULENT BOUNDARY LAYER

P. G. Parikh, W. C. Reynolds, R. Jayaraman, and L. W. Carr
Department of Mechanical Engineering, Stanford University
Stanford, California 94305

Summary

This paper reports experiments on an unsteady turbulent boundary layer. The upstream portion of the flow is steady (in the mean). In the downstream region, the boundary layer sees a linearly decreasing free-stream velocity. This velocity gradient oscillates in time, at frequencies ranging from zero to approximately the bursting frequency. Considerable detail is reported for a low-amplitude case, and preliminary results are given for a higher amplitude sufficient to produce some reverse flow. For the small amplitude, the mean velocity and mean turbulence intensity profiles are unaffected by the oscillations. The amplitude of the periodic velocity component, although as much as 70% greater than that in the free stream for very low frequencies, becomes equal to that in the free stream at higher frequencies. At high frequencies, both the boundary layer thickness and the Reynolds stress distribution across the boundary layer become frozen. The behavior at larger amplitude is quite similar. Most importantly, at sufficiently high frequencies the boundary layer thickness remains frozen at its mean value over the oscillation cycle, even though flow reverses near the wall during a part of the cycle.

Introduction

The objectives of the Stanford Unsteady Turbulent Boundary Layer Program are: to develop a fundamental understanding of such flows, to provide a definitive data base which can be used to guide turbulence model development, and to provide test cases which can be used by computers for comparison with predictions.

Due to space limitations, work of other investigators will not be summarized here, except to note that all the previous experiments are characterized by unsteady flow at the inlet to the unsteady region. For a comparison of the present experimental parameter range with those of other investigations, see Reference 1. The distinctive feature of the present experiments is that the boundary layer at the inlet to the unsteady region is a standard, steady, flat-plate turbulent boundary layer. It is then subjected to controlled oscillations of the free stream. This feature is especially important from the point of view of a computer, who needs precise specification of boundary conditions for computation of the flow.

Free-Stream Boundary Condition of the Present Experiment

The desired free-stream velocity $u_\infty(x,t)$ in the water tunnel built for this work is shown in Fig. 1. u_∞ remains steady and uniform for the first two meters of boundary layer development. It then-decreases linearly in the test section; the magnitude of the velocity gradient varies sinusoidally from zero to a maximum value during the oscillation cycle. The mean free-stream velocity distribution in the test section is thus linearly decreasing and corresponds to the distribution at the cycle phase angle of 90° , while the amplitude of imposed free-stream oscillations grows linearly in the streamwise direction, starting at zero at the entrance to a maximum value of a_0 at the exit. Hence,

$$u_\infty(x,t) = u_{\infty,0} \quad x < x_0$$

$$= u_{\infty,0} - \frac{a_0(x-x_0)}{L} [1 - \cos \omega t], \quad x_0 < x < x_0 + L$$

The important parameters of this problem are the amplitude parameter $a = a_0/u_{\infty,0}$ and the frequency parameter: $\delta_0 = f\delta_0/u_{\infty,0}$. Here $f = \omega/(2\pi)$ and δ_0 is the thickness of the boundary layer at the inlet to the unsteady region. In the present experiments:

$$u_{\infty,0} = 0.73 \text{ m/s}, \quad \delta_0 = 0.05 \text{ m}, \quad 0 < f < 2 \text{ Hz}, \quad 0 < a < 0.25, \quad 0 < \delta_0 < 0.14$$

It should be mentioned that the value of the frequency parameter δ_0 at the so-called "bursting frequency" in turbulent boundary layers is about 0.2 [2]. Thus the imposed oscillation frequencies used in the present experiments cover the range from quasi-steady ($f = 0$) to values approaching the bursting frequency. The results reported here are for two non-dimensional amplitudes, $a = 0.05$ and 0.25 (nominally). The latter is sufficient to cause reverse flow in a turbulent boundary layer at the end of the test section during a part of the oscillation cycle.

Experimental Facility

Figure 2 is a schematic of the facility. The 16:1 nozzle contraction is followed by a 2 m long development section, where the test boundary layer is grown on the top wall. A constant head and a constant flow resistance provide a constant flow. The free-stream velocity in the development section is maintained uniform along x by bleed from the bottom wall.

The linear decrease in free-stream velocity in the test section is accomplished by uniformly bleeding off some flow through the bottom wall in the test section. The remainder of the flow exits downstream. Each of

these two flows exits the tunnel through slots in an oscillating plate. The design ensures that, regardless of the position of the oscillating plate, the total flow area of the slots remains the same. The slots are the controlling resistance of the entire fluid circuit, hence the constant flow. By sinusoidally oscillating the plate, a linearly decreasing periodic free-stream distribution is established in the test section, while the upstream flow in the development section remains steady.

Measurement and Data-Processing Techniques

Pitot tubes are used for mean velocity measurements in steady flow regions. Unsteady velocity measurements use a single-channel, forward-scatter, Bragg-shifted DISA laser anemometer in the tracking mode.

Following Hussain and Reynolds [3], the instantaneous velocity signal from an unsteady turbulent flow may be decomposed into three parts:

$$u = \bar{u} + \tilde{u} + u' \quad (1)$$

where \bar{u} is the mean, \tilde{u} is the time-dependent, organized (deterministic) component, and u' is the random fluctuation. \bar{u} is determined by long-time averaging of u . Here \tilde{u} is of a periodic nature and may be determined by first phase-averaging the instantaneous velocity signal and then subtracting out the mean. Thus,

$$\tilde{u} = \langle u \rangle - \bar{u} \quad (2)$$

Here $\langle u \rangle$, the phase average velocity, is determined by averaging over an ensemble of samples taken at a fixed phase in the imposed oscillation. In the present experiments, with harmonic oscillation of the free stream, the response at points within the boundary layer is almost sinusoidal, with higher harmonics contributing less than 5%. Hence, \tilde{u} may also be extracted from the instantaneous signal u by cross-correlation with a sine wave in phase with the oscillation. A digital correlator (HP 3721A) was used to determine cross-correlations leading to the \tilde{u} data reported here. Currently a BBC MIMIC-11 laboratory minicomputer system is used for automatic data acquisition and processing, allowing the determination of phase averages of u and u'^2 .

The measurements reported here were taken at a fixed streamwise location near the end of the test section at $x - x_0 = 0.306 \text{ m}$.

Behavior at Small Amplitude of Imposed Oscillations

The mean velocity profiles measured with the oscillating plate in fixed positions $\theta = 0, 90^\circ, 180^\circ$ are fit by dashed curves in Fig. 3. These represent phase-averaged profiles at zero frequency, i.e., quasi-steady profiles. At this amplitude ($a = 0.05$), the response of the boundary layer is almost linear, so that the profile corresponding to $\theta = 90^\circ$ lies nearly midway between the $\theta = 0$ and 180° profiles. The 90° profile represents the mean profile for quasi-steady oscillations. The difference between the 0 and 90° profiles at a fixed y -location represents the amplitude of quasi-steady oscillations at that location in the boundary layer. Note that the quasi-steady amplitudes in the boundary layer are larger than the free-stream amplitude.

The mean velocity profiles measured under oscillatory conditions at 0.5 Hz and 2.0 Hz are shown as data points in Fig. 3. Note that the mean velocity profiles at various frequencies are identical with the profile measured under stationary condition with pulsar angle set at $\theta = 90^\circ$. It may be concluded that the mean velocity profile (at a fixed amplitude $a = 0.05$) is independent of the imposed oscillation frequency in the entire range $0 \leq f \leq 2$ Hz. The same behavior persists all the way up to the wall.

This behavior of the mean velocity profile may be explained by an examination of the governing equations. Use of (1) in the momentum equation and time-averaging yields

$$\bar{u} \frac{\partial \bar{u}}{\partial x} + \bar{v} \frac{\partial \bar{u}}{\partial y} = - \frac{1}{\rho} \frac{\partial \bar{p}}{\partial x} + \nu \frac{\partial^2 \bar{u}}{\partial y^2} - \frac{1}{\rho} \frac{\partial}{\partial y} \left[\bar{u}' \bar{v}' + \bar{w}' \bar{v}' \right] \quad (3)$$

Equation (3) may be recognised as the equation governing an ordinary turbulent boundary layer, except for the addition of the term $\bar{w}' \bar{v}'$, which represents Reynolds stresses arising from the organized oscillations.

The time-mean pressure gradient $\partial \bar{p} / \partial x$ may be shown to be independent of the imposed oscillation frequency and the same as that obtained for $f = 0$ at $\theta = 90^\circ$. Therefore, the mean velocity field will be frequency-dependent if and only if one or both of the following happens:

- The distribution of Reynolds stress $\bar{u}' \bar{v}'$ is altered under oscillatory conditions and is dependent on the frequency of forced oscillations.
- The Reynolds stress $\bar{w}' \bar{v}'$ arising from organized fluctuations becomes significant compared with $\bar{u}' \bar{v}'$.

We shall now argue that neither of the above requirements is met. Figure 4 shows the measured distribution of u'_{rms} under stationary condition with the pulser at $\theta = 90^\circ$ (the mean position) as well as those measured under oscillatory conditions at frequencies up to 2 Hz. Note that u'_{rms} is independent of the imposed oscillation frequency and, further, that it is the same as that measured at $f = 0$ and $\theta = 90^\circ$. We believe that the same would be true for $\overline{u'v'}$, which at present we cannot measure. Figure 5 gives a comparison between measured values of $\overline{u'v'}$ at 2 Hz with data on $\overline{u'v'}$ obtained by Anderson [4] in a steady adverse pressure gradient boundary layer at comparable conditions. The present data on $\overline{u'v'}$ were obtained by separate LDA measurements of \tilde{u} and \tilde{v} and their respective phases. It may be seen that the contribution of $\overline{u'v'}$ to total Reynolds stress is insignificant over almost the entire boundary layer. Hence, $\overline{u'v'}$ is independent of frequency and $\overline{u'v'}$ is negligible, and so the mean velocity profile is also independent of frequency and is the same as that found at $f = 0$ with $\theta = 90^\circ$.

The behavior of the periodic component \tilde{u} will next be examined. We denote

$$\tilde{u} = a_1(y) \cos[\omega t + \phi(y)] \quad (4)$$

The profiles of amplitudes a_1 measured in the boundary layer and normalized by the free-stream amplitude $a_{1,\infty}$ are shown in Fig. 6. The profile for quasi-steady ($f = 0$) oscillations was determined, as explained earlier, from the mean velocity profiles measured at $f = 0$ with $\theta = 0^\circ$, 90° , and 180° (see Figs. 3(a), (b)). Note that, during quasi-steady oscillations, the amplitude in the boundary layer exceeds the free-stream amplitude by as much as 70%. It may be mentioned that data for $f = 0.1$ Hz, not shown on Fig. 6, do indeed come very close to the quasi-steady behavior.

As the frequency is increased, the amplitude within the boundary layer is attenuated. The amplitude appears to drop as f is increased and then rises again. At high frequencies, the amplitude in most of the boundary layer is the same as in the free-stream; near the wall the amplitude of the periodic component rapidly drops to zero.

The phase differences between the boundary layer oscillations and free-stream oscillations are shown in Fig. 7. For $f = 0$ there is no phase difference. The largest phase lags in the outer region of the boundary layer were observed at $f = 0.25$ Hz. The effect of increasing the frequency is to reduce the phase lag in the outer region, but to

introduce large phase leads in the region very close to the wall. Clearly, the asymptotic behavior of the outer region for high frequencies is once again a zero phase lag with respect to free-stream oscillations, as in the quasi-steady case.

At high frequencies, the combination of the asymptotic behaviors of $a_1/a_{1,\infty}$ and ϕ in the outer region together with the fact that the mean velocity profile is unaffected by imposed oscillations, has the effect of freezing the boundary layer thickness. This is shown in Fig. 8, where the phase-averaged boundary layer thickness $\langle \delta_{99} \rangle$ is plotted as a function of the cycle phase angle for several frequencies. The quasi-steady behavior of $\langle \delta_{99} \rangle$ is quite obvious: at $\theta = 0$, the boundary layer in the test section continues to develop under a zero pressure gradient and is the thinnest at this point in the entire cycle. As the phase angle is increased, pressure gradients of increasing adversity are imposed on the boundary layer, causing it to thicken. The maximum thickness is attained at $\theta = 180^\circ$ under the maximum adverse pressure gradient. Hence, at $f = 0$, δ oscillates 180° out of phase with u_∞ .

Under oscillatory conditions at $f = 0.25$, 0.5 , and 2.0 hz, two things happen: a significant phase lag develops from quasi-steady behavior and the amplitude attenuates with increasing frequency. For the $f = 2.0$ hz case, the variation over the complete cycle is less than 1% and the boundary layer thickness is practically frozen during the oscillation cycle.

It may be shown by a simple argument based on a mixing length model of boundary layer turbulence that the freezing of the boundary layer thickness at high frequencies is also accompanied by freezing of the Reynolds stress over the oscillation cycle. To prove this, we hypothesize that the phase-averaged Reynolds stress distribution may be related to the phase-averaged velocity profile in the same manner as for a steady boundary layer, i.e.,

$$-\langle u'v' \rangle = c_m \frac{\partial \langle u \rangle}{\partial y}, \quad c_m = \lambda^2 \left| \frac{\partial \langle u \rangle}{\partial y} \right| \quad (5)$$

Now, in the outer region of the boundary layer, the mixing length λ may be modeled as

$$\lambda = \lambda \langle \delta_{99} \rangle \quad (6)$$

where λ is nearly a constant. Now,

$$\langle u \rangle = \bar{u} + \tilde{u} = \bar{u} + a_1(y) \cos(\omega t + \phi(y)) \quad (7)$$

However, in the high-frequency limit,

$$a_1(y) = a_{1,\infty} = \text{const} ; \quad \phi(y) = 0 \quad \text{and} \quad \langle \delta_{.99} \rangle = \overline{\delta_{.99}} = \text{const.} \quad (8)$$

Therefore

$$\frac{\partial \langle u \rangle}{\partial y} = \frac{\overline{u}}{y} \quad (9)$$

Combining the above, one finds

$$-\langle u'v' \rangle = \lambda^2 \left(\overline{\delta_{.99}} \right)^2 \left[\frac{\overline{u}}{y} \right]^2 = -\overline{u'v'} \quad (10)$$

i.e., the phase-averaged Reynolds stress in the outer region also becomes frozen at $-\overline{u'v'}$.

Experimental evidence of this stress-freezing behavior was obtained by measurements of phase-averaged normal turbulent stress $\langle u'^2 \rangle$. The quasi-steady ($f = 0$) profiles of $\langle u'^2 \rangle$ are shown in Fig. 9 for three phase angles $\theta = 0^\circ$, 90° , and 180° . Note that the distribution for 90° lies nearly midway between those for 0° and 180° . The distribution of $\langle u'^2 \rangle$ for 90° is the same as the distribution of $\overline{u'^2}$, as seen earlier. Therefore, the difference between the 0° and 90° curves in Fig. 9 represents the amplitude of quasi-steady oscillations of $\langle u'^2 \rangle$ at any point in the boundary layer. This amplitude was determined graphically from Fig. 9 and is plotted in Fig. 10 for the case of $f = 0$. Under oscillatory conditions, the amplitude of the normal stress oscillations in the boundary layer attenuates as the frequency of imposed oscillations is increased from $f = 0$. At $f = 2.0$ hr, the amplitude of stress oscillations across the boundary layer is almost zero over the outer region, as seen in Fig. 10, i.e., the stress is almost frozen over the oscillation cycle.

Behavior Under Large Amplitudes of Imposed Oscillations

We now discuss the case of $\alpha = 0.25$. All data reported for this case are preliminary and subject to revision. They are included here because of their special interest to this meeting. Also, because of apparatus peculiarities, α varies somewhat with f in this case, hence 0.25 is only a nominal value.

The behavior is qualitatively similar to the $\alpha = 0.05$ case. The mean velocity profiles for $f = 0$, 0.25, 0.5, and 2.0 hr are shown in Fig. 11. Note that the profiles are identical for the cases of $f = 0$, 0.5, and 2.0 hr. For the case of $f = 0.25$, however, there is a

significant deviation in the outer part of the boundary layer. This deviation results from excessive thickening of the boundary layer during a part of the oscillation cycle around the phase angle of 180° . The blockage effect of an excessively thick boundary layer causes an increase in the local free-stream velocity in the test section. Therefore, the desired linearly decreasing free-stream velocity distribution is not achieved over a part of the cycle. At higher frequencies, though, the boundary layer thickness over the entire oscillation cycle deviates very little from its mean value, corresponding to the $\theta = 90^\circ$, $f = 0$ condition.

The behavior of the amplitude ratio and phase difference with respect to free-stream, as shown in Figs. 12 and 13, is quite similar to that for the lower-amplitude case. At high frequency, the overshoot in the amplitude ratio disappears and phase angles over most of the boundary layer approach zero. Very close to the wall, there is a tendency to develop phase leads.

The phase-averaged velocity profiles for $f = 2.0$ hz are shown in Fig. 14. Note that at $\theta = 180^\circ$ there is a small region of reversed flow close to the wall. Despite this flow reversal, the boundary layer thickness remains close to its mean value, as seen in Fig. 15. This behavior is in contrast to that of a steady boundary layer, where excessive thickening of the boundary layer occurs as flow reversal is approached. At low frequency ($f = 0.25$ hz), the thickness oscillates as much as $\pm 40\%$ about the mean value; however, at $f = 2.0$ hz this variation is only about $\pm 5\%$.

Conclusions

The conclusions from our experiments to date may be summarized as follows:

1. The mean velocity profile in the boundary layer is unaffected by imposed free-stream oscillations in the range of frequencies employed, and it is the same as the one measured with a free-stream velocity distribution held steady at its mean value.
2. This behavior of the mean velocity field is a consequence of two observations: (a) the time-averaged Reynolds stress distribution across the boundary layer is unaffected by the imposed oscillations and is indeed the same as the one measured with the free-stream velocity distribution held steady at the mean value; and (b) the Reynolds stresses arising from the organized velocity fluctuations under imposed oscillatory conditions are negligible compared to the Reynolds stresses due to the random fluctuations.

3. The amplitude of the periodic component in the boundary layer under quasi-steady oscillations ($f \neq 0$) is as much as 70% larger than the imposed free-stream amplitude. However, at higher frequencies the peak amplitude in the boundary layer is rapidly attenuated toward an asymptotic behavior where amplitudes in the outer region of the boundary layer become the same as the free-stream amplitude, dropping off to zero in the near-wall region.
4. Quasi-steady boundary layer velocity response is in phase with the imposed free-stream oscillations. As the frequency is increased, phase lags begin to develop in the outer region of the boundary layer. The magnitude of this phase lag reaches a maximum and then decreases with increasing frequency until an asymptotic limit is reached where the outer region once again responds in phase with the free stream. Near the wall, however, large lead angles are present at higher oscillation frequencies.
5. A consequence of (3) and (4) above is that the boundary layer thickness becomes nearly frozen over the oscillation cycle at higher frequencies. This remains true even if flow reversal takes place in the near-wall region over a part of the oscillation cycle, as in the large-amplitude case.
6. A consequence of (3), (4), and (5) above is that the Reynolds stress distribution in the outer region of the boundary layer also becomes frozen over the oscillation cycle at higher frequencies.

Acknowledgments

This research is carried out at Stanford in cooperation with and under the sponsorship of the Army Aeromechanics Laboratory, the NASA-Ames Research Center, and the Army Research Office. The authors wish to express their gratitude to James McCroskey (AML), Mr. Leroy Presley (NASA-Ames), and Dr. Robert Singleton (ARO) for their continued assistance.

References

1. Parikh, P. G., et al.: "On the Behavior of an Unsteady Turbulent Boundary Layer." To appear in Numerical and Physical Aspects of Aerodynamic Flows, Tuncer Cebeci, ed., Springer-Verlag Publishing Co. (1981).
2. Rao, K. N., et al.: "The 'Bursting Phenomenon' in a Turbulent Boundary Layer." *J. Fluid Mech.*, 48, 339-352 (1971).
3. Hussain, A.K.M.F., and Reynolds, W. C.: "The Mechanics of an Organized Wave in Turbulent Shear Flow." *J. Fluid Mech.*, 41, 241-258 (1970), and 54, 241-288 (1972).
4. Andersen, P. S., Kays, W. M., and Moffat, R. J.: "The Turbulent Boundary Layer on a Porous Plate: An Experimental Study of the Fluid Mechanics for Adverse Free-Stream Pressure Gradients." Report No. EMT-15, Dept. of Mech. Engrg., Stanford University (1972).

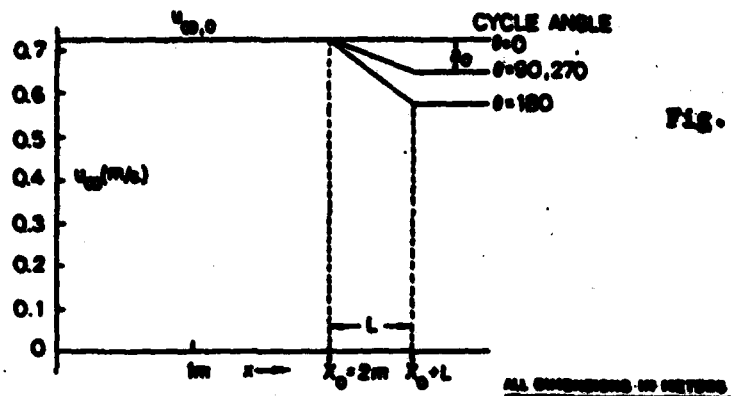


Fig. 1. Pre-stream velocity variation.

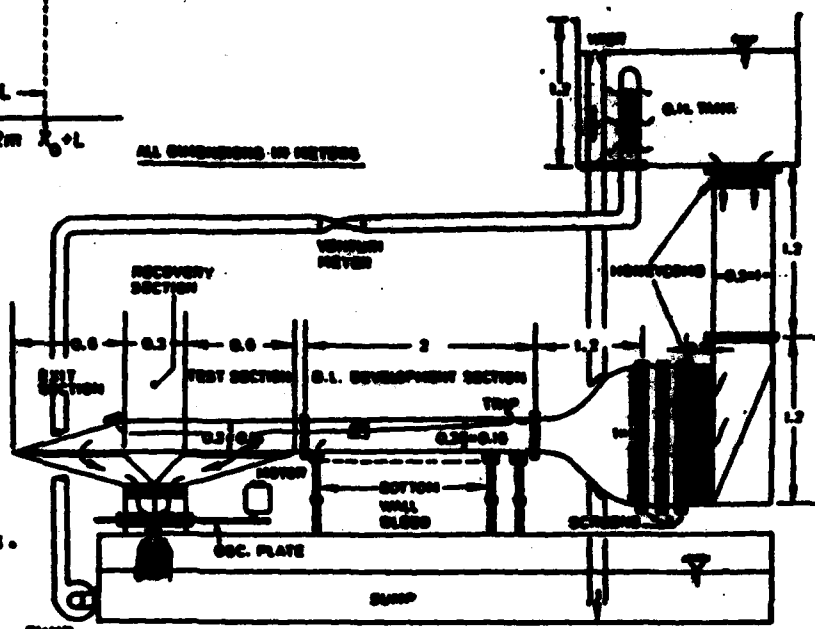


Fig. 2. The apparatus.

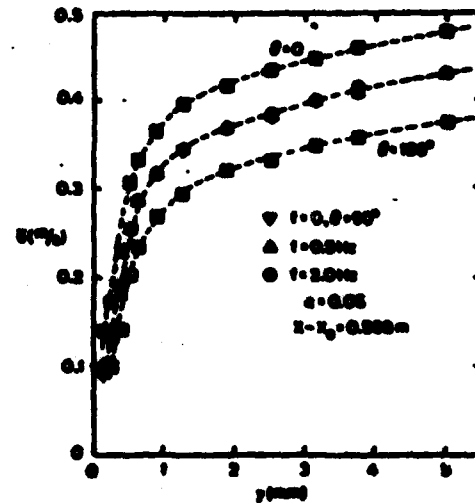
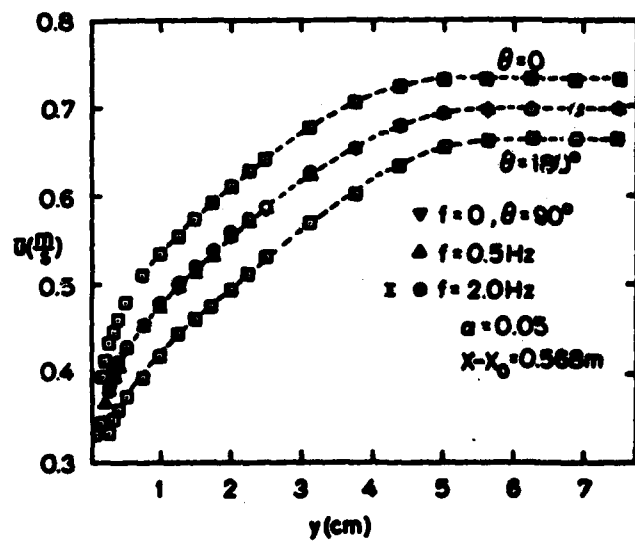


Fig. 3. Mean velocity profiles at three frequencies and profiles at the extremes of the oscillation at zero frequency for $a = 0.05$.

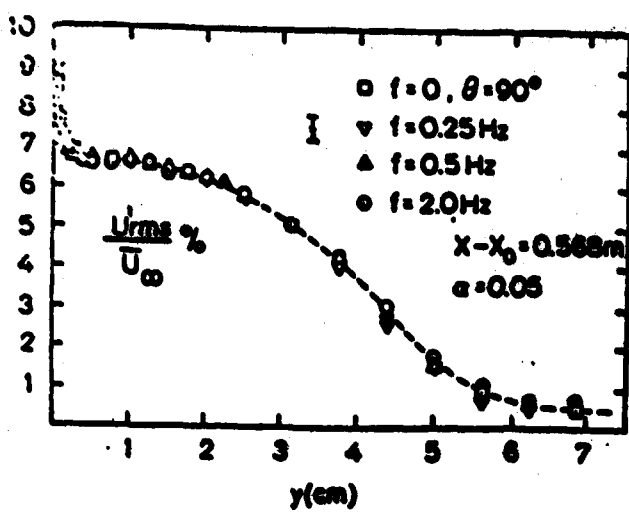


Fig. 4. Mean turbulence profiles for $\alpha = 0.05$.

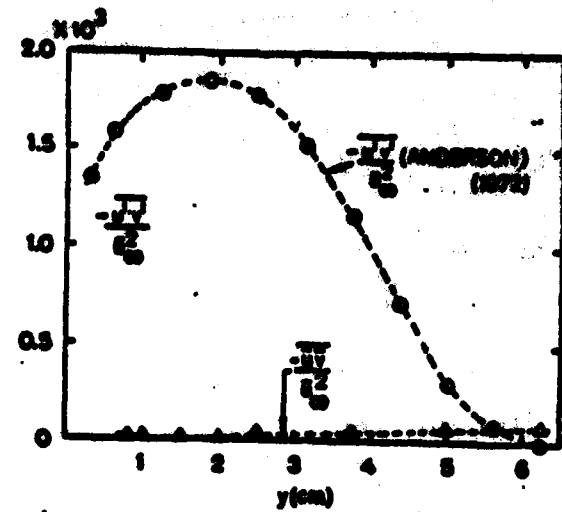


Fig. 5. Turbulent and organised Reynolds stresses for $\alpha = 0.05$.

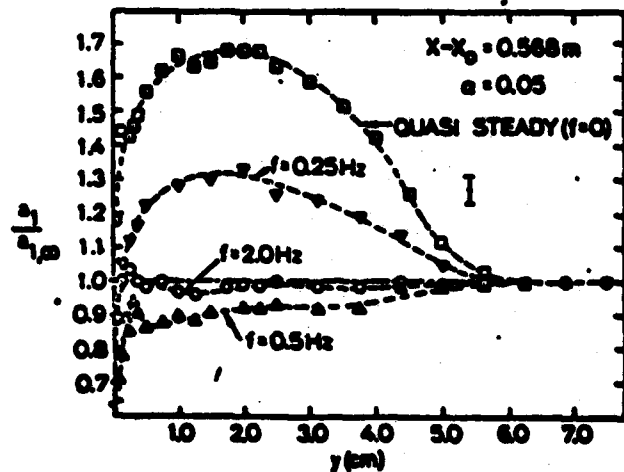


Fig. 6. Amplitude of organized disturbance for $\alpha = 0.05$.

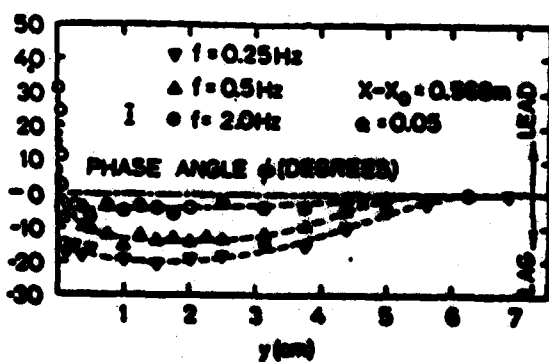


Fig. 7. Phase of organized disturbance for $\alpha = 0.05$.

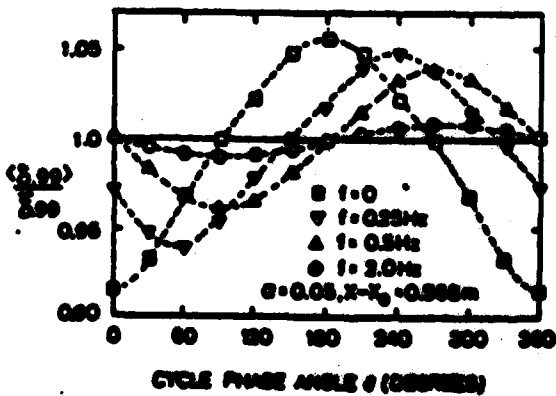


Fig. 8. Boundary layer thickness variation for $\alpha = 0.05$.

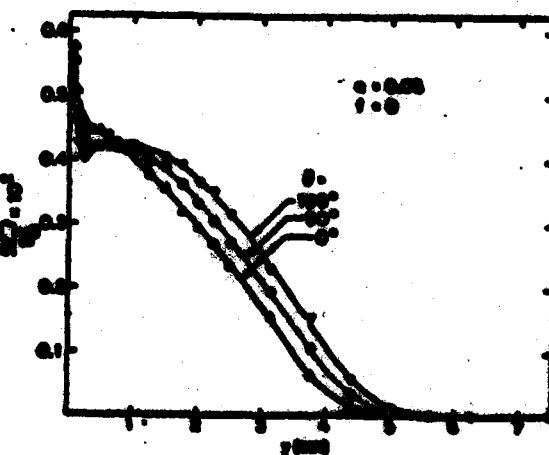


Fig. 9. Phase-averaged longitudinal fluctuation for $\alpha = 0.05$, $f = 0$.

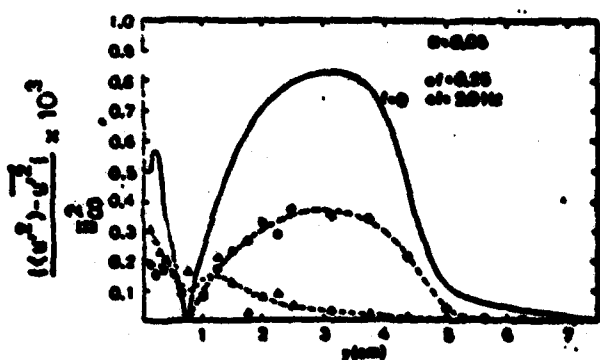


Fig. 10. Reynolds stress oscillations at $\alpha = 0.05$.

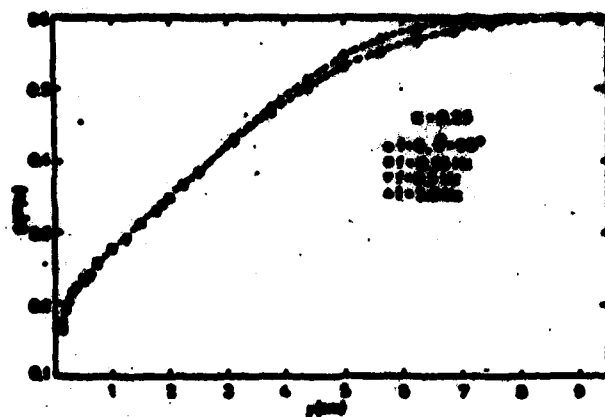


Fig. 11. Mean velocity at $\alpha = 0.25$ (preliminary).

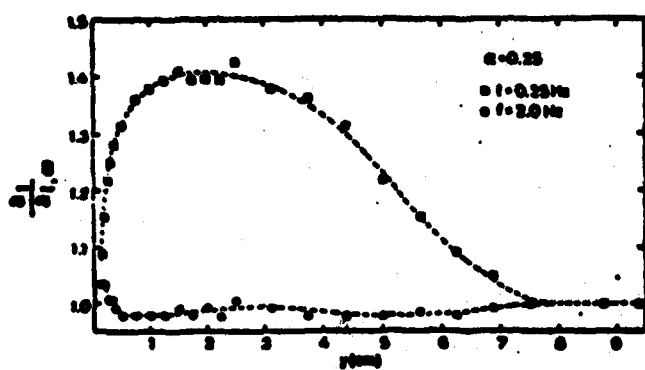


Fig. 12. Amplitude of organized disturbance for $\alpha = 0.25$ (preliminary).

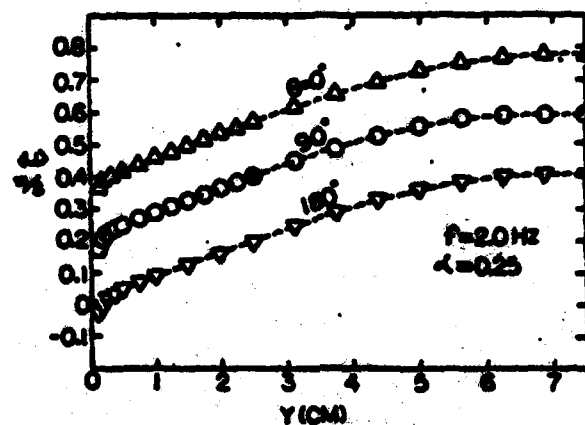


Fig. 14. Phase average velocity profiles for $\alpha = 0.25$ (preliminary).

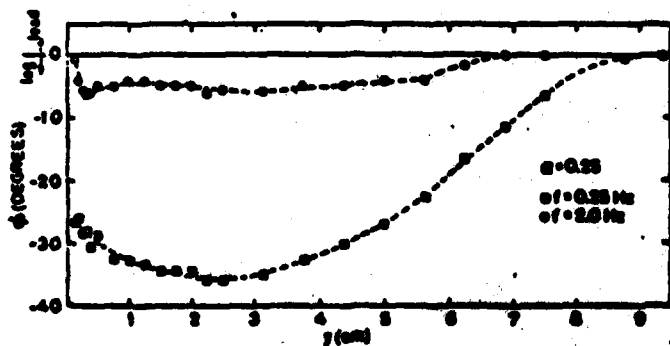


Fig. 13. Phase of organized disturbances for $\alpha = 0.25$ (preliminary).

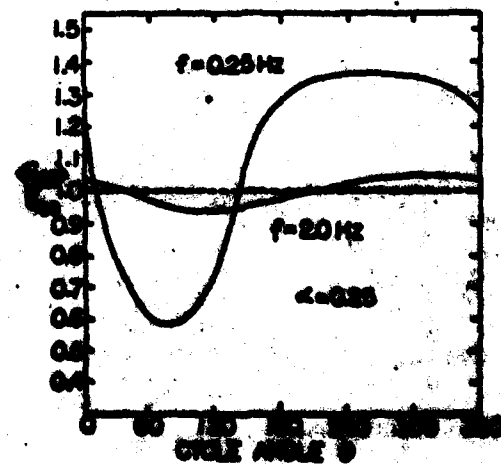


Fig. 15. Boundary layer thickness variation for $\alpha = 0.25$ (preliminary).

1. Report No. NASA TN-81304 USAAVRADCOM TR-81-B-17		2. Government Assumption No. AD-A103 903	
3. Author(s) (18) (19) Dynamic Behavior of an Unsteady Turbulent Boundary Layer			
4. Performer Organization Name and Address Aeros Research Center, NASA, and AVRADCOM Research and Technology Laboratories Moffett Field, CA 94035			
5. Sponsoring Agency Name and Address National Aeronautics and Space Administration, Washington, D.C. 20545, and U.S. Army Aviation Research & Development Command, St. Louis, MO63166			
6. Performance Dates 10/1/81 - 12/31/81			
7. Contract or Grant No. 992-21-01			
8. Report Type and Period Covered Technical memo			
9. Key Word (Suggested by Author(s)) boundary layers, turbulent boundary layer, boundary layer flow, oscillating flow, unsteady flow, pressure gradient			
10. Distribution Statement Unlimited			
11. Security Classif. (of this report) UNCLASSIFIED			
12. Security Classif. (of this page) UNCLASSIFIED			
13. Number of Pages 25		14. Cost \$ 25.00	

NASA FORM

*For sale by the National Technical Information Service, Springfield, Virginia 22161

388090